Vegetable Research

ARTICLE

Open Access

https://doi.org/10.48130/vegres-0024-0027

Vegetable Research **2024**, in press

Fine mapping of QTL-*fl3.1* reveal *SmeFL* as the candidate gene regulating fruit length in eggplant (*Solanum melongena* L.)

Hongtao Pang[1], Jiaqi Ai[1], Wuhong Wang[1], Tianhua Hu[1], Haijiao Hu[1], Jinglei Wang[1], Yaqin Yan[1], Xuexia Wu[2], Chonglai Bao[1*] and Qingzhen Wei[1*]

[1] *Institute of Vegetable, Zhejiang Academy of Agricultural Sciences, Hangzhou 310021, China*
[2] *Horticultural Research Institute, Shanghai Academy of Agricultural Sciences, Shanghai 201403, China*
* Corresponding authors, E-mail: baocl@zaas.ac.cn; weiqz@zaas.ac.cn

Abstract

Eggplant (*Solanum melongena* L.) is an important vegetable crop with abundant variations in fruit morphology, making it a good model for studying fruit development. In this study, quantitative trait loci (QTL) sequencing (QTL-seq) was conducted on multiple F_2 populations, successfully mapping the fruit length-related locus *fl3.1* on eggplant chromosome 3 (E03). Fine mapping further narrowed down this region to 106.6 kb using a large population of 968 F_2 plants. Within this region, a total of eight genes were identified, and *Smechr0302217* (*SmeFL*) was determined to be the most likely candidate gene through validation using RNA-seq and qRT-PCR. Sequence analysis of the parental materials revealed 12 SNPs/InDels in *Smechr0302217*, potentially accounting for the fruit length differences. Combining these findings with further cytological and transcriptomic analyses, we propose that *SmeFL* regulates fruit length by promoting cell expansion in eggplant. The identification of *SmeFL* contributes to a better understanding of the role of microtubule-associated proteins in eggplant fruit development, as well as the mechanism underlying eggplant fruit elongation.

Citation: Pang H, Ai J, Wang W, Hu T, Hu H, et al. 2024. Fine mapping of QTL-*fl3.1* reveal *SmeFL* as the candidate gene regulating fruit length in eggplant (*Solanum melongena* L.). *Vegetable Research* https://doi.org/10.48130/vegres-0024-0027

Introduction

Eggplant (*Solanum melongena* L., 2n=24) is cultivated globally, especially in Asia. According to the latest statistics of the FAO (2020–2022; https://www.fao.org/faostat/en/#home), the cultivation area of eggplants has decreased to 1.89 million hectares, while the yield has increased to 59.31 million tons. The size and shape of eggplant fruits are crucial agronomic traits affecting yield and market value, which also exhibit regional preferences. Thus, it is important to identify the genes responsible for fruit morphological development and understand the regulatory mechanisms involved in eggplant fruit development.

There are four main traits related to fruit size: fruit length (FL), fruit diameter (FD), fruit shape index (FS: FL/FD) and fruit weight (FW). Fruit length directly affects the quality and yield of eggplant and varies greatly among different varieties. The inheritance patterns of FL, FD, FS and FW of eggplant are consistent with those of quantitative traits[1–3]. Three FL QTLs, two FD QTLs, two FS QTLs, and three FW QTLs were detected using F_2 populations derived from a cross between *S. linnaeanum* MM195 and *S. melongena* MM738[4]. Frary et al.[5] conducted composite interval mapping (CIM) analysis for 42 traits using 736 molecular markers, and identified a total of 71 QTLs for 32 phenotypes. Portis et al.[6] performed phenotyping of 20 agriculturally relevant traits using the F_2 population 305E40 × 67/3 planted at two different locations. Six FL QTLs were detected at E01, E02, E03, E07, E08, and E11, with the largest QTLs explaining 17.8% (*flE03*) and 10.1% (*flE11*) of the phenotypic variation, respectively. Four FS QTLs were detected in ML and were located on E01, E03 (2 sites), and E07. Seven FW QTLs were mapped in two locations, among which the major QTL, *fwE02*, was identified from the populations at both locations. Portis et al.[7] analyzed 191 germplasm materials for genome-wide associations and found 4 FL QTLs, 17 FD QTLs, 7 FS QTLs, and 10 FW QTLs. Using the *S. incanum* (MM577) IL population bred in the *S. melongena* (AN-S-26) background, Mangino et al.[8] detected twelve fruit shape index QTLs on chromosomes 2, 3, 4 and 7, which were spread over eight ILs. By comparative transcriptomic analysis, Shi et al.[9] identified the gene *SmOVATE5* (*Smechr0202384*), which negatively affected affect the leaf and silique growth of *Arabidopsis thaliana* by inducing the overexpressing of *SmOVATE5*. This finding suggested that *SmOVATE5* inhibits cell elongation, thereby negatively regulating fruit development. Despite that there are several studies on eggplant fruit length-related traits, no genes have been fine mapped.

In tomatoes, *SUN*, *OVATE*, *LC*, and *FAS* are associated with fruit shape. *SUN* is located on chromosome 7 and serves as a positive regulator in fruit development[10]. The *SUN* mutation is caused by the insertion of a 24.7 kb DNA fragment mediated by a transposon on chromosome 10[11]. This insertion, which results in a repeat, leads to increased expression of *SUN*. The homologous gene *CsSUN* in cucumber has also been implicated in fruit elongation[12]. Although there is research basis for the genes that control fruit length and certain mechanisms of fruit development in other crops, the mechanisms underlying eggplant fruit elongation is still poorly understood.

In the present study, we constructed three F_2 populations for

the QTL detection of eggplant fruit length. The major-effect locus *fl3.1* was stably colocated in different F_2 populations based on the QTL-seq results. A large F_2-3 population was used to narrow down the QTL region to a 106.6 kb region on eggplant chromosome 3, which compromised eight genes. The *SmeFL* gene was identified as the most likely candidate gene for determining eggplant fruit length. Further analysis revealed that the expression of *SmeFL* may alter the direction of cell expansion, suggesting a crucial role for cell expansion-related networks in eggplant fruit development.

Materials and methods

Plant materials and phenotypic analysis

Two different segregating populations were used for quantitative trait locus localization of length traits in eggplant fruits. The F_2 populations were derived from crosses 1811 × 1836 (F_2-1) and 1825 × 1836 (F_2-2). Another F_2-3, which was obtained by crossing 1838 × 1815, was used for fine mapping. The parental lines displayed diverse fruit characteristics in terms of shape. *S. melongena*-1811 has round fruits measuring approximately 4 cm centimeters in length. In contrast, 1815 has oval-shaped fruits, each approximately 9 cm in length. The fruits of 1825 are oblate in shape, with a length of approximately 15 cm. In contrast, 1836 has long barrel-shaped fruits that are approximately 35 cm in length. 1838 has fruits with a clear linear shape, approximately 40 cm in length.

The experimental materials were cultivated at the Qiaosi Experimental Base of Zhejiang Academy of Agricultural Sciences using a ridge planting system, with single-row planting and a row spacing of 20–25 cm. Flowers were hand-pollinated at 2-3 nodes and tagged. Two QTL-seq populations were planted in the spring of 2018. The fine mapping population was planted in the spring of 2023. Fruit length was determined when fruits were fully mature at 40 days after pollination (DAP). To determine the time point at which rapid fruit elongation occurred, 10 plants of 1838 and 10 plants of 1815 with good growth were selected for continuous length and diameter measurements. For data collection, three representative fruits were selected as standards from each plant, and their individual fruit lengths were measured. Subsequently, the average fruit length was calculated for each plant using the measurements of the three selected fruits. The statistical analysis of the data in this study was all performed using Excel 2016 and GraphPad Prism V8.0.

Paraffin sections

Ovaries or eggplant fruits at 0, 4, 8, 12, 16, 20, 30, and 40 DAP from 1838 and 1815 plants were fixed in formalin–acetic acid–alcohol (50%) and then they were embedded in paraffin; Paraffin sections were cut on a Leica RM2016 microtome (Leica, Shanghai, China). The sections were incubated in safranin O staining solution for 2 h and then rinsed with tap water to remove excess dye. The slides were placed in 50%, 70%, and 80% alcohol for 3-8 seconds for decolorization. Sections were soaked in plant solid green staining solution for 6-20 seconds and dehydrated with anhydrous ethanol twice for 5 minutes. The sections were placed into three cylinders of xylene for 5 min. Finally, the tissue sections were mounted with neutral balsam. Finally, the sections were observed and photographed with a Nikon Eclipse E100 microscope (Nikon Corporation, Tokyo, Japan). The cell number and cell area were calculated from images using Fiji (National Institutes of Health, Bethesda, MD, USA, https://imagej.net/Fiji).

QTL mapping

We applied QTL-seq to two F_2 (F_2-1 and F_2-2) populations in this study, and the preliminary QTL mapping results of F_2-3 were combined[13]. Equal amounts of DNA from 16 individuals with extremely long fruits and 16 with extremely short fruits were selected from 106 F_2-1 plants to construct the L-1 pool and S-1 pool, respectively. The L-2 pool and S-2 pool composed of 20 individuals with extremely long and extremely short fruits, respectively, were constructed from 139 F_2-2 plants using equal amounts of DNA. Young leaves were collected from three parents and two F_2 populations and frozen in liquid nitrogen. Genomic DNA was extracted using the CTAB method. The extracted DNA was tested by electrophoresis in a 1% agarose gel, analyzed on a NanoPhotometer® spectrophotometer (IMPLEN, CA, USA) and measured using a Qubit® DNA Assay Kit in a Qubit® 2.0 Fluorometer (Life Technologies, CA, USA) for concentration and purity. The qualified library was sequenced on a Illumina HiSeq™ PE150 platform. The original image data generated by the sequencer were converted into sequence data via base calling (Illumina pipeline CASAVA v1.8). A quality control procedure was then applied to the image data to remove unusable reads, including those containing the Illumina library construction adapters or more than 10% unknown bases (N bases), and those with one end having more than 50% low-quality bases (sequencing quality value≤5). The effective sequencing data were compared to the reference genome by BWA software, and the comparison results were removed by SAMtools. SNP and InDel polymorphisms were detected by GATK3.8 and annotated by ANNOVAR (2013 Aug 23). The HQ-1315 gene dataset[13] was used for gene annotation.

Fine mapping of FL

Combined with the initial QTL mapping results for fruit length in three F_2 populations of eggplant, fine mapping was carried out using a large F_2-3 segregating population. The DNA extraction method was the same as that described in QTL mapping. First, markers were developed within the initial localization interval, linkage groups were constructed with 19 markers in 290 plants, and then recombinants were screened in 968 plants. Insertion-deletion (InDel) markers were developed in the target region from the QTL-seq results of 1838 and 1815. Based on the phenotypic and genotypic data of the 968 plants from the F_2-3 population, a linkage map was constructed with QTL IciMapping 4.2 software.

RNA-seq

Transcriptomic analyses were performed on three biological replicates of whole eggplant fruit samples (without a style and calyx) collected at four developmental stages (0, 4, 8 and 12 DAP) from 1838 (L) and 1815 (S). Three technical replicates were performed for each biological replicate. Samples were rapidly frozen in liquid nitrogen and stored at −80 °C. RNA sequencing was performed as described by Yang et al.[14]. Total RNA was isolated with an RNAprep Pure Plant Kit (DP441) (Tiangen Biotech Co., Ltd., Beijing, China). RNA purity was determined using a Nanodrop 2000 (NanoDrop Technologies, USA) and the A260/A280 ratios of all the samples were approximately 2.0. RNA integrity was detected using an Agilent 2100 Bioanalyzer. Three biological replicates were subjected to for

RNA-seq, and sequenced using the Illumina NovaSeq 6000 platform with in paired-end 150 bp mode. To obtain high-quality clean reads, the raw reads were filtered by fastp (v0.20.0). Using HISAT2 (v2.1.0), paired-end clean reads were mapped to the *S. melongena* reference genome (*S. melongena* HQ-1315 genome). For each transcription region, the fragments per kilobase of transcript per million mapped reads (FPKM) value was calculated by using StringTie software. Differentially expressed genes (DEGs) were annotated using the Kyoto Encyclopedia of Genes and Genomes (KEGG) and Gene Ontology (GO) databases.

Content determination of IAA, CTK, and GA_3

Auxins (IAA), cytokinins (CTK), gibberellins (GA_3) were measured in eggplant fruits. ELISA kits were used to determine the endogenous levels of IAA, CTK, and GA_3 in 1838 and 1815 at four stages via the double-antibody sandwich method. Fruits of 1838 and 1815 were sampled on the day of flowering (unpollinated), 4, 8 and 12 days after pollination. Remove the calyx from the fruits and wrap it in aluminum foil before freezing it in liquid nitrogen for freezing, and then placed in the refrigerator at −80 °C for reserve. The endogenous phytohormone levels in different developmental periods of the samples were determined by using the enzyme immunoassay kit of plant growth hormone (IAA), enzyme immunoassay kit of plant cytokinin (CTK), enzyme immunoassay kit of plant gibberellin 3 (GA_3), and the kits were supplied by Nanjing JixiHuiyuan Biological Science and Technology Co. Phyto hormone content was detected based on the AB SCIEX QTRAP® 6500. Three biological replicates were analyzed for each treatment group.

Results

Phenotypic analysis of the mapping populations

Three F_2 populations were constructed by the following crosses: 1811 × 1836 (F_2-1), 1825 × 1836 (F_2-2), and 1838 × 1815 (F_2-3) (Fig. 1a). A total of 106 and 139 plants were obtained for F_2-1 and F_2-2 populations, respectively. For F_2-3, a large population composed of 968 plants was obtained. Phenotypic data from F_2-1 and F_2-2 indicated that fruit length and diameter

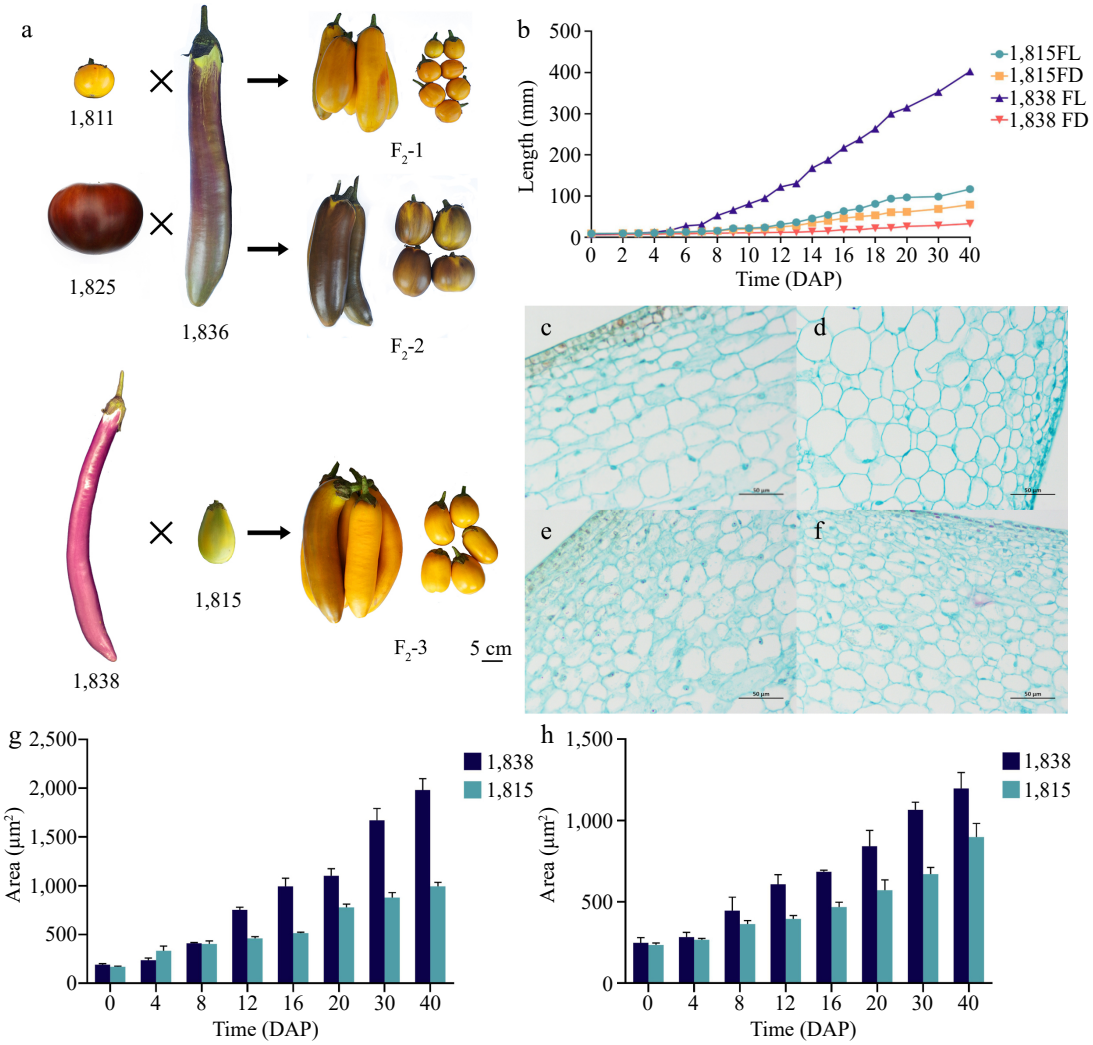

Fig. 1 Fruit length phenotypic analysis of five parents and selected extreme-fruit length individuals of three F_2 populations (bar = 5 cm). (a) Parents of three QTL populations and extreme individual plants of F_2 at 40 DAP. (b) Fruit length and diameter statistics of 1838 and 1815. (c, d) Longitudinal and transverse sections of fruit cells of 1838 at 12 DAP. (e, f) Longitudinal and transverse sections of fruit cells of 1815 at 12 DAP. (g, h) Comparison of the longitudinal and transverse cell area in 1838 and 1815.

were continuously segregated and normally distributed (Supplemental Fig. S1). The results suggested that there was considerable variation in FL and FD among the F_2 populations, which was consistent with the quantitative trait, making these populations appropriate for QTL analysis. The statistical analysis of the F_2-3 parents showed that at 0 DAP, the fruit length of 1815 was 0.90 cm, with a diameter of 0.95 cm, indicating more of a spherical shape. In contrast, the fruit of 1838 was more elongated, with a length of only 0.79 cm and a diameter of 0.61 cm. At 40 DAP, the lengths of the 1838 and 1815 fruits were 40 cm and 11 cm respectively, and the difference in average fruit length increased to 29 cm. The differences in fruit length became apparent at 4 DAP, and the growth rate of 1838 peaked at 8 DAP (Fig. 1b).

To determine the underlying cytological basis for fruit length elongation, paraffin sections of 1838 and 1815 fruits at 0, 4, 8, 12, 16, 20, 30 and 40 DAP were analyzed (Fig. 1c-f, Supplemental Fig. S2). At 0 DAP, the transverse section of 1838 had 26 cells per unit area (1×10^4 μm^2) and the longitudinal section had 32 cells per unit area (1×10 μm^2). The transverse section of 1815 had 34 cells per unit area (1×10^4 μm^2) and the longitudinal section had 44 cells per unit area (1×10^4 μm^2). The mean cell area of 1838 was 190 μm² in longitudinal sections at 0 DAP, which was larger than that of 1815 (167 μm^2). In transverse sections, both 1815 and 1838 had similar cell areas of approximately 240 μm^2. However, contrary to the phenotype shown, the cell area of 1838 was always larger than that of 1815 in transverse sections. At 12 DAP, the mean cell area of 1838 was 751.84 μm^2, while that of 1815 was 460.85 μm². After 12 DAP, the difference in mean cell area between 1838 and 1815 became large (Fig. 1g, h). In conclusion, the cellular distribution of 1838 was lower than that of 1815, both longitudinally and transversely. Therefore, the elongation of 1838 fruit was likely resulted from the longitudinal elongation of cells. The observed increase in fruit diameter may be attributable to the enlargement of transversely oriented cells. However, the larger cells of 1838 may not be sufficient to compensate for the disparity in the number of transversely arranged cells compared to that of 1815, consequently contributing to the disparity in fruit diameter. The size and shape of the cells were similar in the early stages until 8 DAP. In the longitudinal section, the longitudinal cell length of 1838 was already longer than that of 1815, although their cell areas were similar at 8 DAP. In the transverse section, the number of cells in 1838 was lower than in 1815. After 8 DAP, the cell area of 1838 was greater than that of 1815. Therefore, phenotypic differences are caused by differences in the longitudinal elongation of cells and the distribution of horizontal cell number.

QTL-seq analysis

To identify the QTLs related to eggplant fruit length, we performed QTL-sequencing using four bulked pools with extremely long/short phenotypes, namely, the L-1 pool, S-1 pool, L-2 pool, S-2 pool, as well as the two paternal lines. A total of 106.07 Gb and 111.46 Gb of clean data were obtained from the F_2-1 and F_2-2 populations, respectively. QTL-seq generated 21.41 Gb (16.24×), 21.12 Gb (14.58×), 32.04 Gb (25.14×), and 31.51 Gb (22.74×) of raw data for 1811, 1836, L-1 and S-1, respectively. L-2, S-2 pools and 1825 yielded 24.15 Gb (18.99×), 33.27 Gb (26.50×), and 32.63 Gb (26.04×) of raw data, respectively (Table S1). After removing low-quality SNPs and InDels, 720,034 and 310,742 SNPs/InDels were obtained for the Δ All-index and ED algorithm calculations, respectively. Sliding window analysis was applied to All-index plots with a 1 Mb window size and 1 kb increment. The 95% confidence level was selected as the screening threshold after 1000 permutation tests (Fig. 2). Based on a 99% confidence interval (Table 1), a major-effect QTL was found at the end of chromosome 3, within a 13.21 Mb region (75.05-88.26 Mb) in F_2-1 and a 23.20 Mb region (64.22-87.42 Mb) in F_2-2. The region of the major-effect QTL in F_2-3 was 71.29-78.26 Mb in our previous study[13]. In addition, two minor-effect QTLs were also identified on chro-

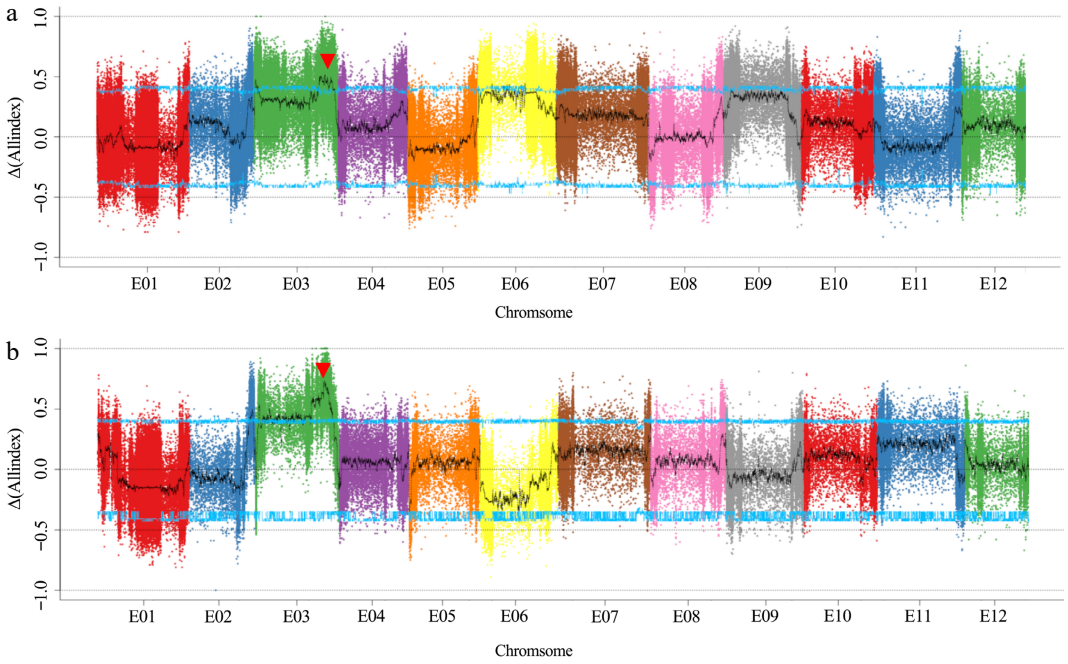

Fig. 2 Δ All-index mapping of fruit length QTLs in F_2-1 and F_2-2, where the blue line represents the 95% threshold.

Table 1. QTLs detected in the mapping populations.

population	Chr.	QTL	Start (bp)	End (bp)	Confidence interval
F_2-1	E03	*fl3.1*	75049001	88261000	99
F_2-2	E02	*fl2.1*	71623001	71907000	99
F_2-2	E03	*fl3.2*	3597001	4470000	99
F_2-2	E03	*fl3.1*	64218001	87415000	99
F_2-3	E03	*fl3.1*	71286001	78262000	99

mosome 2 and at the starting position of chromosome 3.

Fine mapping of *fl3.1*

The overlap region of the three preliminary mapping intervals for *fl3.1* was 75.05–78.26 Mb. To avoid neglecting genes that might be outside the overlap interval, we expanded the fine mapping interval by 5 Mb (70.05–83.26 Mb). According to the colocalization results, we developed 298 markers based on the QTL-seq results of F_2-3 for InDel variations. Among them, 86 makers exhibited stable polymorphic amplification between the two parents and the F_2 individuals. A genetic map was constructed using 19 equally distributed markers (Supplemental Table S2) with clear bands and 290 F_2-3 individuals (Fig. 3a). The total length of the linkage map was 66.11 cM, corresponding to 72.04–82.59 Mb in E03. The average genetic distance between the markers was 3.48 cM and the average physical distance was 0.56 Mb. The major-effect QTL was located in the 15.66 cM region between InDel 58 and InDel 66. This region corresponds to the 568 kb physical interval of E03: 82,024,192 bp-82,591,943 bp.

To further fine map the QTL region, six additional easy-to-distinguish InDel markers were developed within the 82.02–82.88 Mb region in E03 (Fig. 3b). Nine InDels were used to construct a genetic map for QTL mapping of *fl3.1* using the F_2-3 population containing 968 individuals (Supplemental Table S3). The linkage map was 6.89 cM in length. A major-effect QTL was mapped to a 1.12 cM region between InDel 61 and InDel 64, and the LOD score was 31.33 (Supplemental Fig. S3), which could explain 13.89% of the phenotypic variation. A total of 31 effective recombinant individuals were identified (Fig. 3c). The physical location of *fl3.1* was finally narrowed to a 106.06 kb region (E03: 82,222,982-82,329,608) (Fig. 3d).

Candidate gene analysis of *fl3.1*

According to the 'HQ-1315' eggplant genome database (http://eggplant-hq.cn/Eggplant/home/index), eight predicted genes were annotated in the 106.6 kb region. These genes included one defective in meristem silencing 3 protein, one structural maintenance of chromosomes flexible hinge domain-containing protein GMI1, one beta-galactosidase, one AP2/ERF and B3 domain-containing transcription factor, one protein IQ-DOMAIN 1, and one soluble starch synthase (Table 2). To determine whether there are differences in the homologous gene *Smechr0302217* of *SUN* gene sequence, we sequenced two parents 1838 and 1815. There was one synonymous mutation in the CDS region of *Smechr0302217*, and 11 SNPs/InDels were found in the promoter. One SNP (T to C) was detected in CDS, but the SNP caused no amino acid changes. Notably, the InDel at position −2192 bp and the SNP at position −1925 contributed to one less BOX4 and a lack of the CGTCA-motif in 1815, respectively. Moreover, the SNP at −1064 bp also produced another TATA-BOX in 1815. (Fig. 3e).

Transcriptome analysis

To investigate the transcriptomic differences related to the molecular mechanism of fruit elongation in eggplant, comparative transcriptome analysis of eggplant fruits was subsequently conducted to identify DEGs at 0, 4, 8 and 12 DAP between 1838 (L) and 1815 (S) (Fig. 4a). A total of 160.43 Gb of data was obtained. The amount of clean data for each sample was no less than 5.92 Gb, and the percentage of Q30 bases was greater than 91.93% (Supplemental Table S4). Ten comparisons (S0 vs. S4, S4 vs. S8, S8 vs. S12, L0 vs. L4, L4 vs. L8, L8 vs. L12, S0 vs. L0, S4 vs. L4, S8 vs. L8, and S12 vs. L12) were performed, which included the same cultivar under different DAPs and samples of different cultivars (1838 and 1815) at the same DAP point. Combined with the fine mapping results and divergent gene expression levels of RNA-seq results (Fig. 4b), we identified *Smechr0302217* as the most likely candidate gene controlling fruit length and verified it via qRT-PCR (Fig. 4c; Supplemental Table S2). The results showed that the relative expression of *Smechr0302217* in 1838 was nearly 5-fold greater than that in 1815 at 12 DAP. This coincided with the period of cell elongation in the section analysis.

After calculating the FPKM values, we identified the DEGs based on the threshold criteria of an $|\log_2 FC| \geq 1$ and a p-value ≤ 0.05. A total of 38472 DEGs were annotated. According to Fig. S4, L0 vs. L4 showed the most significant difference in DEG number, and the number of upregulated genes was greater than that of downregulated genes. The results showed that the differentially expressed genes were most abundant in the early stage of fruit development (Supplemental Fig. S4), which may be a critical period affecting cell number and cell expansion. A Venn diagram of the L-group and S-group showed 248 and 179 common DEGs, respectively. There were 424 common DEGs in the S0 vs. L0, S4 vs. L4, S8 vs. L8, and S12 vs. L12 comparisons, which may be related to fruit development. These common genes may be closely related to the development of eggplant fruit (Fig. 4d-f).

The DEGs among different comparison groups were annotated (Supplemental Table S5). Based on the KEGG analysis, we

Table 2. The information of genes in fine mapping region

Gene ID	Position	Gene annotation
Smechr0302211	82225171-82225560	Protein defective in meristem silencing 3
Smechr0302212	82226053-82234339	—
Smechr0302213	82245138-82280629	Protein GMI1
Smechr0302214	82290277-82291199	Beta-galactosidase 9
Smechr0302215	82291354-82291908	—
Smechr0302216	82295773-82298371	AP2/ERF and B3 domain-containing transcription factor
Smechr0302217	82302722-82306030	Protein IQ-DOMAIN 1
Smechr0302218	82314017-82328336	Soluble starch synthase 1

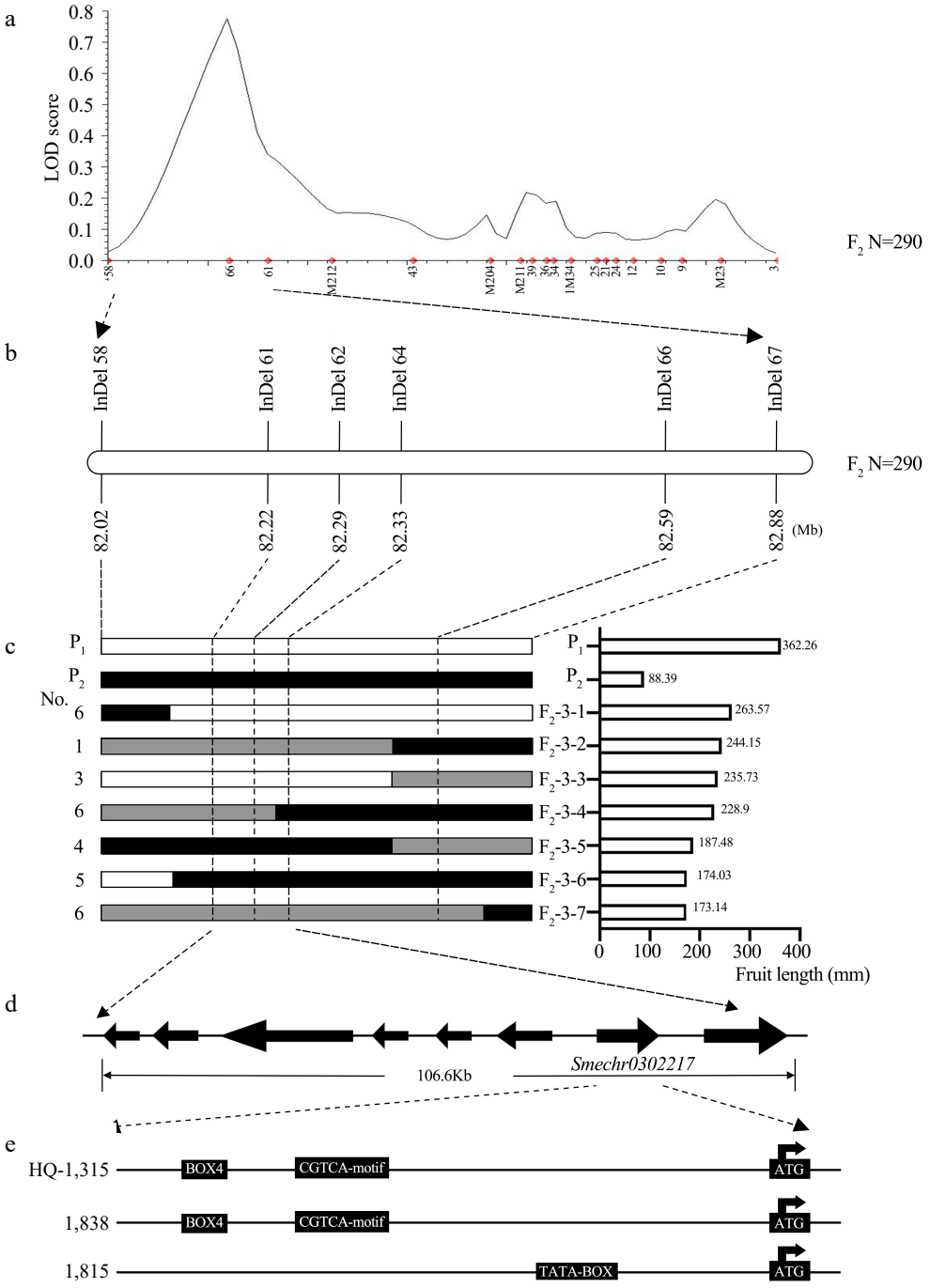

Fig. 3 Fine mapping of *fl3.1*. a Fine mapping based on 290 F_2 individual plants. b *fl3.1* was mapped to a 568 kb region between the InDel 58 and InDel 66 markers. c The numbers on the left indicate the number of recombinants. The white filled and black bars represent segments homozygous for the 1838 and 1815 alleles, respectively. Fruit length is shown for the recombinant plants (3-F_2-1-7) and parents on the right. d Eight genes in the 106.6 kb region. e Three promoter element differences according to sequencing analysis.

compared the two groups at the same stage. The Plant hormone signal transduction, Photosynthesis, and MAPK signaling pathways-plants were the most highly enriched pathways. GO analysis suggested differences in terms associated with photosynthesis, plant-type hypersensitive response, defense response, and cell wall organization during fruit development. Furthermore, according to the GO analysis of L and S at the same DAP (Supplemental Fig. S5), there was significant enrichment in the auxin, ethylene and gibberellin metabolism pathways. The metabolic pathways of cell wall components such as lignin, pectin, and hemicellulose were also highly enriched. Metabolic pathway enrichment of cell wall components such as xyloglucan, lignin, and pectin metabolism was greater in the L group than in the S group, and similar results were also observed for the cellular mitosis pathway and microtubule movement with vesicular transport along microtubules. Thus, greater activity in endogenous hormone-mediated cell wall metabolism, microtubule movement and cell division is

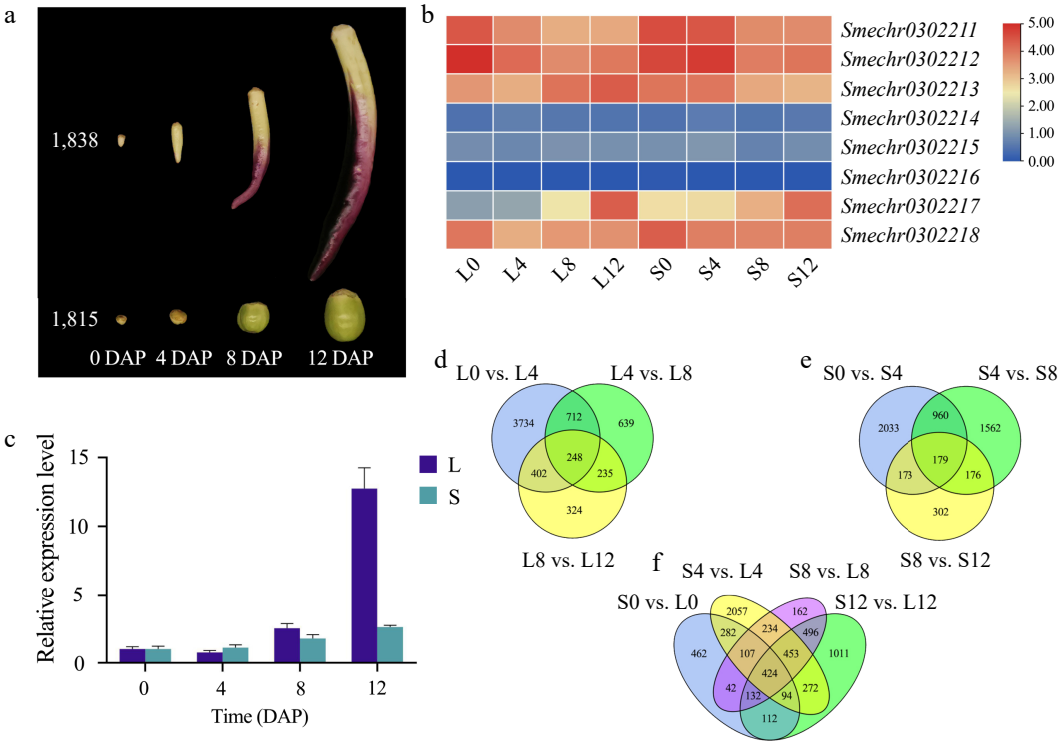

Fig. 4 RNA-seq samples and data analysis a Four sampling periods of RNA-seq samples. b Heatmap of 8 genes. c qRT-PCR results for *Smechr0302217*. d-f Venn diagram of the ten comparison groups.

likely responsible for the differences in fruit length in eggplant. The fruit shape differences between 1838 and 1815 might be contributed to microtubules related processes.

Measurement of plant hormones

The growth and development of fruits are closely related to cell proliferation and expansion, processes that are regulated by hormones such as auxins, cytokinins, gibberellins, and abscisic acid[15]. Cell division and expansion are inseparable from the control of hormones. The IAA concentration in 1838 at 0 and 4 DAP was approximately 0.1 μg/g lower than that in 1815, with little difference at 8 DAP, but the IAA content in 1838 is slightly higher than that in 1815 at 12 DAP (Fig. 5a). The CTK concentration in 1838 was 0.1 μg/g higher than that in 1815 at 0 DAP, but was 0.2 μg/g lower than that in 1815 at 12 DAP. The CTK concentrations of both were almost the same at 0 and 8 DAP (Fig. 5b). The GA_3 content of 1838 was 1 ng/g greater than that of 1815 at 0 and 12 DAP, with a little differences at 4 and 8 DAP (Fig. 5c). Different IAA and GA_3 levels may allow more cellulose microfibrils to remain transverse, and a higher CTK content may promote the effect on the reorientation of cellulose microfibrils from a transverse to a longitudinal orientation.

Discussion

Fruit length is an important factor affecting the appearance, quality and yield of eggplant. However, no gene has been fine mapped in eggplant. Therefore, understanding the genetic basis of fruit length is important for eggplant breeding and cultivar improvement. In this study, QTL-seq was performed using three F_2 populations, and major-effect QTLs related to fruit length were detected at the end of chromosome 3 with intervals of 75.05-88.26 Mb in F_2-1 (Fig. 2a), 64.22-87.42 Mb in F_2-2 (Fig. 2b), and 71.29-78.26 Mb in F_2-3 (Wei et al. 2020). Using traditional mapping methods, we constructed a genetic linkage map for the large F_2-3 population. Eventually, the QTL region of *fl3.1*was narrowed down to a candidate interval of 106.6 kb (Fig. 3). In previous studies, one *fl*, eight *fd*, three *fs*, and four *fw* loci were shown to be located near this position, and the gene *Smechr0301963* was predicted to be a possible

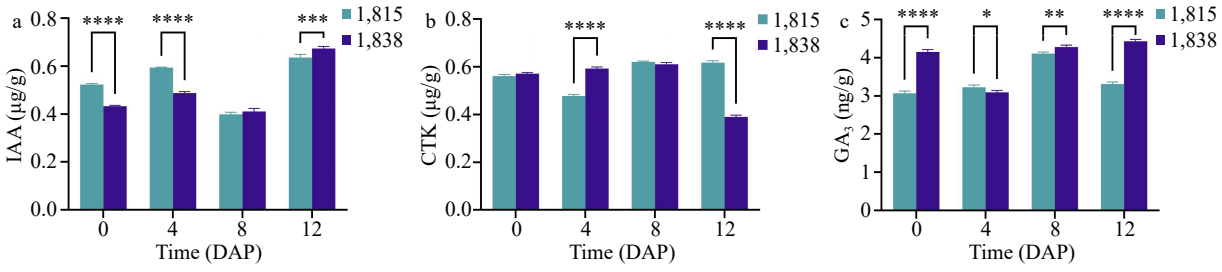

Fig. 5 Expression assay of IAA, CTK and GA_3. a-c IAA, CTK and GA_3 expression at 0, 4, 8, and 12 DAP in 1838 and 1815

key gene affecting fruit elongation[6,7,13].

Fruit development in plants is usually divided into two stages, with cell division primarily occurring early in fruit development, followed by cell stretching until the size and shape of the final fruit are settled[16–19]. Many studies have focused on these two stages and suggested that cell number and cell size are important determinants of final fruit size[20,21]. In this study, morphological and cytological analyses revealed differences in the number of cells per unit area between 1838 and 1815 at 0 DAP (Fig. 1). However, there was no significant difference in the average cell area per unit area between 1838 and 1815. After 12 DAP, the longitudinal cell size of 1838 differed from that of 1815, and at later DAP stages, the cell size of 1838 was significantly larger than that of 1815. Because of the fruit formation characteristics of 1838, the number of cells at other stages was not counted. This suggests that longitudinal cell elongation of 1838 fruit cells during the cell extension stage is the main factor contributing to fruit elongation.

By combining the results of fine mapping and gene annotation analysis, we identified the tomato *SlSUN11* homologous gene *Smechr0302217* as a candidate gene that controls eggplant fruit elongation. The *SmeFL* (*Smechr0302217*) was located on chromosome 3, with a length of 3309 bp, including 4 CDS, encoding the IQD1 protein composed of 470 amino acids. This gene was highly expressed at 12 DAP, which was consistent with the results of phenotypic analysis. There have been many reports on homologous *SUN* genes in tomato. The *SUN*-encoded IQD protein contains a plant-specific structural domain of 67 conserved amino acid residues called the IQ67 domain[10]. Reverse transcription transposon mediated gene replication leads to the upregulation of *SUN* gene expression, resulting in morphological variation in tomato fruits[11,22]. *SUN* controls tomato shape by increasing cell division in the longitudinal direction and decreasing cell division in the transverse direction of the fruit[23]. This suggests that changes in cell division patterns are critical to *SUN*-mediated fruit shape changes, which is consistent with the findings of our paraffin section analysis. A total of 34 *SlSUN*, 31 *SlOFP* and 9 *SlYABBY* genes were identified in tomato, and their expression patterns in different tissues and developmental stages were analyzed using RNA-seq. Compared with those in other tissues, the expression of *SlSUN10* was greater at 10 days post anthesis[24]. This finding is consistent with the RNA-seq and qRT-PCR results of *smechr0302217*(Fig. 4b, c). Nonetheless, *SUN* may also regulate ovary shape by effecting the expression of other genes such as those involved in growth hormone signaling and actin cytoskeletal organization[25]. During the process of cellular expansion, plant cell wall plays a bifunctional role by concurrently serving as a structural scaffold for plant cells and providing elastic encapsulation for cellular expansion. Over the course of cellular expansion, heightened cellular metabolic activities contribute to the energy necessary for cell growth[26]. Cellular expansion encompasses two distinct processes: first, a reduction in intracellular osmotic potential leading to cellular imbibition and expansion; second, softening and relaxation of the cell wall, involving the incorporation of new cell wall constituents such as cellulose, hemicellulose, pectin, etc., for structural reconstitution[27]. The synergistic coordination of these processes is essential for maintaining the normal expansion of cells. In the present study, transcriptome analysis revealed that photosynthesis and cell wall metabolism were more active in 1838, and that a greater energy supply with softening and relaxation of the cell wall provided favorable conditions for cell elongation (Supplemental Fig. S5). Cellulose microfibrils are a fibrous component of the cell wall, and can constrain cell expansion in one direction and control cell elongation[28,29]. Mutants of microtubule-associated genes exhibit phenotypic defects and alterations in organ size, suggesting that microtubules are also involved in the regulation of cell elongation and are associated with altered anisotropic cell growth[30–32]. Cortical microtubules attach to the cell membrane and direct the movement of cellulose synthesis complexes. These cellulose synthesis complexes push the cellulose microfibrils toward the cell wall. Transversely arranged microtubules provide a binding force that is more suitable for cell elongation[33,34]. Thereby, the candidate gene *SmeFL* possibly regulates the orientation of cellulose microfibers and impacts the direction of cell expansion in eggplant.

Studies of *Arabidopsis* and rice have shown that the IQD protein that involved in calcium signaling can directly bind microtubules and is a key regulator of organ shape[35]. Ca^{2+} is an important secondary messenger during plant growth and development, controlling microtubule (MT) array passage to determine the direction of cell expansion. The Ca^{2+} signaling pathway plays a key role in determining plant cell morphogenesis[36,37]. High levels of auxin increase Ca^{2+} levels, resulting in a greater affinity between calmodulin (CAM) and IQD, thus making it easier for SPR2 to bind to the minus ends of MT and increasing the stability of branching and the dynamicity of the MT architecture[38]. Clevenger et al.[39] reported that *SUN* indirectly leads to strong changes in the expression of genes involved in processes related to cell division, the cell wall and patterning through calcium signaling, thus affecting fruit shape. Bürstenbinder et al.[40] localized IQD1 in the MT cytoskeleton, and overexpression of selected IQD proteins altered cellular MT, which provides CAM-dependent Ca^{2+} signaling integration platform proteins to regulate cell shape and growth. The NET3C-KLCR1-IQD2 module, which acts as an actin-microtubule bridging complex, has a direct influence on endoplasmic reticulum (ER) morphology and the structure of ER-PM contact sites[41]. These results suggest that the *SmeFL* gene is also likely to be localize to the MT cytoskeleton, affecting fruit shape through cellular microtubules and being regulated by hormones.

The *SUN* gene is associated with various complex mechanisms involved in the regulation of fruit morphology. Various hormones, including cytokinins, gibberellins, abscisic acid, and ethylene, play roles in cell expansion[42]. In this study, differences in different fruit phenotypes were observed from at 8 DAP, and *SmeFL* also began to show differential expression. Moreover, the difference was more obvious at 12 DAP with greater differences in *SmeFL* expression and variations in gibberellin content. Enrichment analysis revealed active photosynthesis and cell wall metabolism during this period. Moreover, the *smeFL* gene, at the same stage, exhibited significant differences in expression levels. IQD proteins, as calcium-binding proteins, can directly bind to microtubules, influencing the orientation of microtubule arrays. They control the direction of cell elongation in the early stages of cell expansion, exerting a lasting impact on organ development. These results suggest that *SmeFL* serves as a crucial factor influencing cell elongation, thereby playing a significant role in eggplant fruit elongation.

Conclusions

In this study, three F_2 populations were utilized to map the QTLs controlling eggplant fruit length. The gene *Smechr0302217* (*SmeFL*) was determined to be the most likely candidate gene through validation using RNA-seq and qRT-PCR. Sequence analysis of the parental materials revealed 12 SNPs/InDels in *SmeFL* potentially accounting for the phenotypic differences. Combining these findings with those of cytological and transcriptomic analyses, we propose that *SmeFL* regulates fruit length by promoting cell expansion in eggplant. The identification of *SmeFL* contributes to a better understanding of the role of microtubule-associated proteins in eggplant fruit development, as well as the mechanism underlying eggplant fruit elongation.

Author contribution statement

Hongtao Pang and Jiaqi Ai participated in conducting the experiments and wrote the manuscript. Wuhong Wang, Tianhua Hu and Haijiao Hu managed experimental materials and recorded phenotypic data. Hongtao Pang, Yaqin Yan, Jinglei Wang and Xuexia Wu participated the experiment, and contributed to the data analysis. Chonglai Bao and Qingzhen Wei initiated the project and contributed the overall research direction. All authors reviewed the results and approved the final version of the manuscript.

Data availability

The datasets generated during the current study are available from the corresponding author Qingzhen Wei (weiqz@zaas.ac.cn) on reasonable request.

Acknowledgments

This work was supported by the Zhejiang Provincial Natural Science Foundation of China (LY23C150003), Youth Program of National Natural Science Foundation of China (32002055), the New Variety Breeding Project of the Major Science Technology Projects of Zhejiang (2021C02065-1-3).

Conflict of interest

The authors declare that they have no conflict of interest.

Supplementary Information accompanies this paper at (XXXXXX)

Dates

Received 20 April 2024; Accepted 24 June 2024; In press 28 June 2024

References

1. Akpan NM, Ogbonna PE, Onyia VN, Okechukwu EC, Dominic II, et al. 2017. Genetic Control and Heterosis of Quantitative Traits in Several Local Eggplant Genotypes. *Notulae Scientia Biologicae* 9(4):520–24
2. Mistry C, Kathiria KB, Sabolu S, Kumar S. 2016. Heritability and gene effects for yield related quantitative traits in eggplant. *Annals of Agricultural Sciences* 61(2):237–46
3. Uddin MS, Billah M, Afroz R, Rahman S, Jahan N, et al. 2021. Evaluation of 130 Eggplant (*Solanum melongena* L.) Genotypes for Future Breeding Program Based on Qualitative and Quantitative Traits, and Various Genetic Parameters. *Horticulturae* 7(10):376
4. Doganlar S, Frary A, Daunay MC, Lester RN, Tanksley SD. 2002. Conservation of gene function in the solanaceae as revealed by comparative mapping of domestication traits in eggplant. *Genetics* 161(4):1713–26
5. Frary A, Frary A, Daunay MC, Huvenaars K, Mank R, et al. 2014. QTL hotspots in eggplant (*Solanum melongena*) detected with a high resolution map and CIM analysis. *Euphytica* 197(2):211–28
6. Portis E, Barchi L, Toppino L, Lanteri S, Acciarri N, et al. 2014. QTL mapping in eggplant reveals clusters of yield-related loci and orthology with the tomato genome. *PLoS One* 9(2):e89499
7. Portis E, Cericola F, Barchi L, Toppino L, Acciarri N, et al. 2015. Association mapping for fruit, plant and leaf morphology traits in eggplant. *PLoS One* 10(8):e0135200
8. Mangino G, Vilanova S, Plazas M, Prohens J, Gramazio P. 2021. Fruit shape morphometric analysis and QTL detection in a set of eggplant introgression lines. *Scientia Horticulturae* 282(7):110006
9. Shi S, Li D, Li S, Wang Y, Tang X, et al. 2023. Comparative transcriptomic analysis of early fruit development in eggplant (*Solanum melongena* L.) and functional characterization of *SmOVATE5*. *Plant Cell Rep* 42(2): 321-36
10. Abel S, Savchenko T, Levy M. 2005. Genome-wide comparative analysis of the *IQD* gene families in *Arabidopsis thaliana* and *Oryza sativa*. *BMC* 5:72
11. Xiao H, Jiang N, Schaffner E, Stockinger EJ, van der Knaap E. 2008. A retrotransposon-mediated gene duplication underlies morphological variation of tomato fruit. *Science* 319(5869):1527–30
12. Pan Y, Liang X, Gao M, Liu H, Meng H, et al. 2017. Round fruit shape in WI7239 cucumber is controlled by two interacting quantitative trait loci with one putatively encoding a tomato *SUN* homolog. *Theor Appl Genet* 130(3):573–86
13. Wei Q, Wang J, Wang W, Hu T, Hu H, et al. 2020. A high-quality chromosome-level genome assembly reveals genetics for important traits in eggplant. *Hortic Res* 7(1):153
14. Yang M, Zhu L, Pan C, Xu L, Liu Y, et al. 2015. Transcriptomic analysis of the regulation of rhizome formation in temperate and Tropical Lotus (*Nelumbo nucifera*). *Sci Rep* 5:13059
15. Xie Y, Liu X, Sun C, Song X, Li X, et al. 2023. *CsTRM5* regulates fruit shape via mediating cell division direction and cell expansion in cucumber. *Hortic Res* 10(3):007
16. Gillaspy G, Ben-David H, Gruissem W. 1993. Fruits: A Developmental Perspective. *Plant Cell* 5(10):1439–51
17. Zhang C, Tanabe K, Wang S, Tamura F, Yoshida A, et al. 2006. The impact of cell division and cell enlargement on the evolution of fruit size in *Pyrus pyrifolia*. *Ann Bot* 98(3):537–43
18. Xiao H, Radovich C, Welty N, Hsu J, Li D, et al. 2009. Integration of tomato reproductive developmental landmarks and expression profiles, and the effect of *SUN* on fruit shape. *BMC Plant Biol* 9:49
19. Eldridge T, Łangowski Ł, Stacey N, Jantzen F, Moubayidin L, et al. 2016. Fruit shape diversity in the Brassicaceae is generated by varying patterns of anisotropy. *Development* 143(18):3394–406
20. Baldazzi V, Valsesia P, Génard M, Bertin N. 2019. Organ-wide and ploidy-dependent regulation both contribute to cell-size determination: evidence from a computational model of tomato fruit. *J Exp Bot* 70(21):6215–228
21. Mauxion JP, Chevalier C, Gonzalez N. 2021. Complex cellular and molecular events determining fruit size. *Trends Plant Sci* 26(10):1023–38
22. Jiang N, Gao D, Xiao H, van der Knaap E. 2009. Genome organization of the tomato *sun* locus and characterization of the unusual retrotransposon *Rider*. *The Plant journal* 60(1):181–93
23. Wu S, Xiao H, Cabrera A, Meulia T, van der Knaap E. 2011. *SUN* regulates vegetative and reproductive organ shape by changing

cell division patterns. *Plant Physiol* 157(3):1175–86
24. Huang Z, Van Houten J, Gonzalez G, Xiao H, van der Knaap, E. 2013. Genome-wide identification, phylogeny and expression analysis of *SUN, OFP* and *YABBY* gene family in tomato. *Mol Genet Genomics* 288(3-4):111–29
25. Wang Y, Clevenger JP, Illa-Berenguer E, Meulia T, van der Knaap E, et al. 2019. A comparison of *sun, ovate, fs8.1* and auxin application on tomato fruit shape and gene expression. *Plant Cell Physiol* 60(5): 1067-81
26. EVANS J R. 2013. Improving photosynthesis. *Plant physiology* 162(4):1780–93
27. COSGROVE D J. 2024. Structure and growth of plant cell walls. *Nat Rev Mol Cell Biol* 25(5):340–58
28. Baskin TI. 2005. Anisotropic expansion of the plant cell wall. *Annu Rev Cell Dev Biol* 21:203–222
29. Cosgrove DJ. 2016. Plant cell wall extensibility: connecting plant cell growth with cell wall structure, mechanics, and the action of wall-modifying enzymes. *J Exp Bot* 67(2):463–76
30. Thitamadee S, Tuchihara K, Hashimoto T. 2002. Microtubule basis for left-handed helical growth in *Arabidopsis*. *Nature* 417(6885):193–96
31. Stoppin-Mellet V, Gaillard J, Timmers T, Neumann E, Conway J, et al. 2007. *Arabidopsis* katanin binds microtubules using a multimeric microtubule-binding domain. *Plant Physiol Biochem* 45(12):867–77
32. George K, Ivan LI, Miroslav OK, Despina S, Olga A, et al. 2017 Katanin Effects on Dynamics of Cortical Microtubules and Mitotic Arrays in *Arabidopsis thaliana* Revealed by Advanced Live-Cell Imaging. *Front Plant Sci* 8: 866
33. Lloyd C. 2011. Dynamic microtubules and the texture of plant cell walls. *Int Rev Cell Mol Biol* 287:287–329
34. Chan J (2012) Microtubule and cellulose microfibril orientation during plant cell and organ growth. *J Microsc* 247(1): 23-32
35. Li Q, Luo S, Zhang L, Feng Q, Song L, et al. 2023. Molecular and genetic regulations of fleshy fruit shape and lessons from *Arabidopsis* and rice. *Hortic Res* 10(7):108
36. Li J, Wang X, Qin T, Zhang Y, Liu X, et al. 2011. MDP25, a novel calcium regulatory protein, mediates hypocotyl cell elongation by destabilizing cortical microtubules in *Arabidopsis*. *Plant Cell* 23(12):4411–27
37. Qin T, Li J, Yuan M, Mao T. 2012. Characterization of the role of calcium in regulating the microtubule-destabilizing activity of MDP25. *Plant Signal Behav* 7(7):708–10
38. Wendrich JR, Yang BJ, Mijnhout P, Xue HW, Weijers D. 2018. IQD proteins integrate auxin and calcium signaling to regulate microtubule dynamics during *Arabidopsis* development
39. Clevenger JP, Van Houten J, Blackwood M, Rodríguez GR, Jikumaru Y, et al. 2015. Network Analyses Reveal Shifts in Transcript Profiles and Metabolites That Accompany the Expression of *SUN* and an Elongated Tomato Fruit. *Plant Physiol* 168(3):1164–78
40. Bürstenbinder K, Möller B, Plötner R, Stamm G, Hause G, Mitra D, Abel S. 2017. The IQD Family of Calmodulin-Binding Proteins Links Calcium Signaling to Microtubules, Membrane Subdomains, and the Nucleus. *Plant Physiol* 173(3):1692–1708
41. Zang J, Klemm S, Pain C, Duckney P, Bao Z, et al. 2021. A novel plant actin-microtubule bridging complex regulates cytoskeletal and ER structure at ER-PM contact sites. *Curr Biol* 31(6):1251–60
42. Bashline L, Lei L, Li S, Gu Y. 2014. Cell wall, cytoskeleton, and cell expansion in higher plants. *Mol Plant* 7(4):586–600